Uncertainty Assessment of Fault Networks in 3D Geologic Models of Mountain Tunnels

A. Krajnovich[1], W. Zhou[1] and M. Gutierrez[2]
[1]*Department of Geology and Geological Engineering, Colorado School of Mines, Golden, CO, USA*
[2]*Department of Civil and Environmental Engineering, Colorado School of Mines, Golden, CO, USA*
E-mail: akrajnov@mines.edu

ABSTRACT: 3D geologic models are applied to predict the location and geometry of fault zones intersecting tunnel alignments in hard rock settings. The modelled fault zones inherit subjective (i.e., epistemic) and objective (i.e., aleatory) uncertainty from the various modelling inputs used, including observations and interpretations. An input-based, uncertainty propagation approach is developed to assess the geologic model uncertainty based on four modelling inputs – surface trace, structural orientation, fault zone thickness and vertical termination depth. The rationale behind selecting and parameterizing probability distributions to characterize the uncertainty of each modelling input based on available data and geologic prior knowledge is discussed. The approach – implemented using open-source code and commercial geologic modelling software – can be applied to a wide range of 3D geologic models in structurally-controlled hard rock settings for a realistic assessment and visualization of uncertainty.

KEYWORDS: 3D Geologic Model, Geologic Prediction, Hard Rock Tunneling, Uncertainty, Unexpected ground conditions

1. INTRODUCTION

Three-dimensional (3D) geologic models are becoming the state of the art for the prediction and communication of subsurface geology in subsurface engineering projects. However, geologic models are often treated as deterministic despite the fact that they are affected by numerous sources of uncertainty stemming from their input data, prior information used and the nature of the modelling method (Caers, 2011; Wellmann & Caumon, 2018). Unexpected ground conditions in tunnelling projects are often a leading cause of cost and schedule overruns and cannot be sufficiently anticipated by a single, deterministic geologic model. Understanding the uncertainty of a 3D geologic model not only provides a measure of model quality to the end user (e.g., tunnel engineers), but also aids the geologist during model creation by analysing the quality of input data and highlighting the impacts of the use of prior knowledge and/or interpretations.

A new, best practice for incorporating new observations of subsurface geology into a preliminary geologic model is proposed that assesses the model against new data probabilistically, using uncertainty as a guide for adapting the initially uncertain model. Traditionally, this assessment is made by an on-site geologist relying on their experience and expertise to interpret new ground conditions revealed by excavation. Implementing a quantitative workflow for assessing and updating geologic model uncertainty provides a powerful tool for both aiding the geologist in predicting subsurface conditions and enhancing how the dynamic understanding of subsurface geology is communicated throughout a tunnelling project.

Geologic uncertainty includes not only objective (i.e., aleatory) sources of uncertainty (e.g., imprecise observations and natural variability of geologic features), but also subjective (i.e., epistemic) uncertainty resulting from incomplete knowledge of the subsurface (Bond, 2015). As opposed to geostatistical methods which focus on spatial variability, Monte-Carlo uncertainty propagation (MCUP) is useful for assessing the impact of geologic uncertainty arising from the various types of geologic modelling inputs, including observations and interpretations (Wellmann & Caumon, 2018). In combination with flexible, implicit geologic modelling algorithms, MCUP allows for creating multiple realizations of an initial geologic model based on perturbations of uncertain modelling inputs. Likelihood and information entropy are calculated from the set of model realizations to visualize the geologic model uncertainty.

2. MODELING IMPLEMENTATION

Applying the MCUP approach to geologic model uncertainty assessment begins with the deliberate selection and characterization of geologic modeling inputs. Focusing the modelling efforts on a clear and important aspect of geology ensures that the uncertainty formulation is realistic and that the geologic model is useful to the tunneling project.

Fault zones – comprised of a network of interconnected fault surfaces bounding varying degrees of fractured and altered rock – introduce zones of compromised geotechnical strength and/or permeability into the surrounding intact rock. In the tectonically uplifted, crystalline rock setting of most mountain tunnels, fault zones are of primary concern to construction (Robinson et al., 1974), requiring a detailed understanding of the location and geometry of their intersection with the tunnel alignment.

In the subsurface, fault zones have complex, 3D geometry which must be approximated from limited information at the surface and supplemented with prior knowledge. A modelling approach using four inputs – surface trace, structural orientation, fault zone thickness and vertical termination depth – is proposed to approximate fault zone geometry using a rectangular slab centred around a fault surface extending from the surface outcrop to an interpreted depth in the subsurface. Figure 1 shows a schematic of a fault zone, highlighting the various sources of uncertainty affecting each modelling input used.

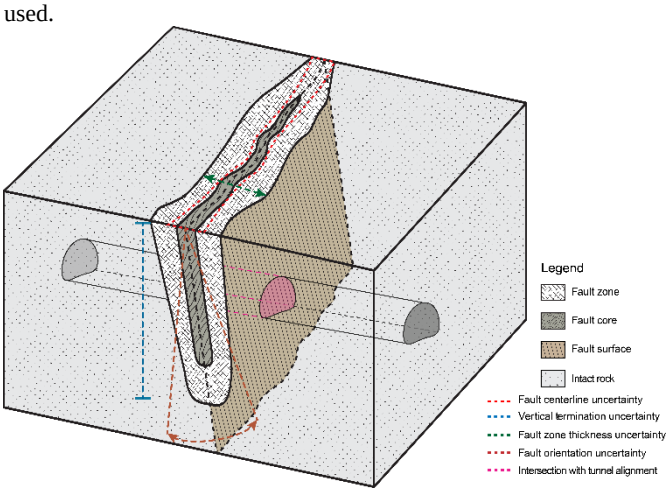

Figure 1. Schematic showing various sources of geologic uncertainty affecting the 3D modelling of fault zones.

The method with which a geologic model is created governs the final quality and realism of the model. This is particularly true for input based MCUP formulations, where a clear workflow translating model inputs to the modelled geologic structure is required for automated generation of model realizations. A workflow for modelling the 3D geometry of fault zones is proposed that retains the

essential geological aspects of the fault zone while providing enough generalization for implementation in MCUP. The fault surface is first modelled from the fault trace (polyline) and a structural orientation (dip and dip direction) (Figure 2(a)). The fault surface is terminated against a horizontal surface at a pre-defined depth (Figure 2(b), and a volume is extruded from the terminated fault surface to define the 3D fault zone (Figure 2(c)).

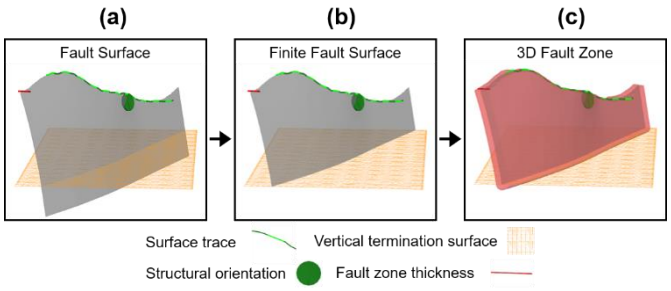

Figure 2. Proposed workflow for modelling the 3D geometry of fault zones in the subsurface.

2.1 Treatment of Uncertainty

Identifying and quantifying the sources of uncertainty affecting the geologic model begins with a careful consideration of the data available and geologic prior knowledge required to characterize each modelling input. Objective uncertainties are typically associated with observations and are therefore straightforward to characterize directly from the data, for example calculating the average and variance of the random deviations of a geologic compass. On the other hand, uncertainties associated with interpretations made during the modelling process are subjective and require the geologist to use prior knowledge to distil down the interpretation to its core reasoning. Parameterization of the geologic prior knowledge is an essential step in quantifying the subjective uncertainty (Wood & Curtis, 2004).

Upon identifying and quantifying the uncertainty sources affecting each geologic modelling input, probability distributions of various types are available to use in the MCUP formulation (Tarantola, 2005). Selecting the – or the set of – appropriate probability distributions for each input is based on the level and type of information available.

2.1.1 Surface Trace

In ideal conditions, the surface trace mapped in the field would follow the centreline of the fault zone and reach along the entire length of the fault. In reality, the definition of the centreline of a fault zone is inconsistent (Torabi et al., and reliance on digitized geologic maps introduces additional uncertainty. Characterizing the uncertainty of the fault trace for modelling, therefore, involves perturbing the shape and location of the trace according to these sources.

The perturbation applied to the fault trace is based on the joint uncertainty of the sources mentioned. The uncertainty regarding the fault zone centreline is quantified by treating the expected fault zone thickness as a 95% confidence interval on the location of the fault zone centreline. Eq. (1) converts the confidence interval to a standard deviation (σ) and characterizes a normal distribution with mean (μ) for the scalar variable x.

$$\sigma = \frac{CI_{95\%}}{3.92}$$
$$P(x|\mu,\sigma) = \frac{1}{\sqrt{2\pi\sigma^2}} \exp\left(-\frac{(x-\mu)^2}{2\sigma^2}\right) \tag{1}$$

The uncertainty of a fault trace drawn from a geologic map has two primary components: geographical and mapping errors. Geographical errors, arising from digitization and conversion between coordinate reference systems, can be estimated using established metrological studies (e.g., Zhong-Zhong, 1995). Mapping errors are more epistemic in nature and are inherent to the original geologic map itself. The method the map was created (e.g., hand drawn vs. computer-aided vector graphics) and any interpretations made by the mapper (e.g., connecting a fault trace between two outcrops) are relevant. Field verification of the map data is one possible way to quantify these errors. Lacking a new mapping effort, field verification can provide an estimate of the error for some known structures, which can then be applied to the dataset as a whole.

2.1.2 Structural orientation

Often characterized using a single dip and dip direction vector, the structural orientation of fault zones inherits a wide range of uncertainties including natural variability of the fault surface, imprecise measurements, measurement bias from difficulty interpreting fault slip surfaces and reliance on regional structural analysis. While the objective sources of uncertainty are treated effectively with large sample sizes, the subjective uncertainty resulting from measurement bias and the use of regional geologic knowledge require a unique formulation to properly characterize the information available for modelling.

Quantifying the uncertainty of the structural orientation used for modelling begins with determining the data available. If sufficient measurements (> 25) of a single fault zone's orientation are available, the uncertainty can be calculated directly by computing the symmetrical orientation matrix of the data (Fisher et al., 1987). Lacking sufficient data, prior knowledge should be leveraged to approximate the expected orientation and/or uncertainty of the modelled structure. For example, regional geologic studies can provide qualitative information on expected fault orientations (e.g., NNW to NE-striking, steeply dipping) that the modeller can convert to reasonable uncertainty ranges for their project.

Pakyuz-Charrier et al. (2018**)** demonstrated that spherical distributions are necessary for appropriately characterizing uncertainty of structural orientation data. The Bingham distribution (Bingham, 1964) is a spherical probability distribution which, depending on its parametrization, can characterize a wide range of levels of uncertainty about the structural orientation of a fault zone. Distribution shapes ranging from spherical uniform to girdle and unimodal can be achieved by varying the relative magnitude of the eigenvalues (λ_i) in Eq. (2).

$$P(\boldsymbol{x}|A) = \exp\left(-\sum_{i=1}^{p-1} \lambda_i x_i^2\right) \frac{1}{c(A)},$$
$$c(A) = \int_{x \in S^{p-1}} exp\left(-\sum_{i=1}^{p-1} \lambda_i x_i^2\right) dS^{p-1}(\boldsymbol{x}) \tag{2}$$

Note that the Bingham distribution is naturally bimodal, and the application of a lower-hemisphere stereographic projection reduces the distribution to a unimodal shape. The Bingham distribution is capable of expressing disparate levels of information regarding the uncertainty in the dip angle and dip direction of a modelled structure. This is particularly useful when modelling with limited information, for example a geologic map with a well-defined fault trace and only a single dip measurement (Figure 3).

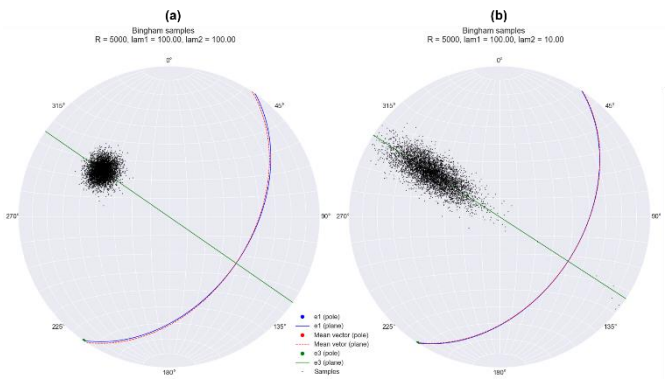

Figure 3. Isotropic (a) vs. anisotropic (b) Bingham distributions.

2.1.3 Vertical Termination Depth

While often modelled as surfaces cutting through the entire volume of the 3D geologic model, faults are finite, terminating at some depth in the subsurface as the displacement along them reduces to zero. The vertical termination depth is particularly important to tunnelling

projects as it may control whether a problematic fault zone intersects the alignment or not. The full extent of the fault zone in the subsurface is rarely observed and must be approximated using prior knowledge relating observations of the fault at the surface and regional geology to the expected termination depth.

The theory of the fault ellipse (Barnett et al., 1987; Schultz & Fossen, 2001) has been demonstrated as an effective approximation of the 3D geometry of faults in various settings. The theory relates the length of a fault along strike to the height of the fault along dip using an aspect ratio (Eq. (3)).

$$Aspect\ ratio = \frac{F_{length}}{F_{height}} \tag{3}$$

Recent work by Torabi et al. (2019**)** utilizing 3D seismic data noted high variability in the aspect ratio for faults (1.5 to 16) due to various factors including mechanical stratigraphy and stress fields variations. The uncertainty of the aspect ratio can therefore at best be characterized using a bounded uniform distribution (Eq. (4)). Typically, mechanical stratigraphy results in larger aspect ratios compared to isotropic rock conditions.

$$P(x|a,b) = \begin{cases} 1/b-a, & for\ a \le x \le b \\ 0, & for\ x<a\ or\ x>b \end{cases} \tag{4}$$

In addition to aspect ratio uncertainty, the vertical termination depth inherits uncertainty from the persistence of the fault trace at the surface. Lacking specific information on the location of fault tip points, an assumption of length must be made using the persistence of a fault trace at the surface as a proxy for F_{length}. Given that abrupt fault trace terminations due to overburden or inaccessibility may be present, the persistence of the fault trace is assigned an uncertainty using a normal distribution based on the observed variability of trace length for faults from the same family.

Horizontal terminations are not considered in the current study as their relevance to tunnel construction is less prevalent than that of vertical terminations. The interested reader is recommended to works applying stochastic simulation to fault-fault interactions (e.g., Aydin & Caers, 2017; Cherpeau et al., 2010**)**.

2.1.4 Fault Zone Thickness

Peacock et al. (2016**)** detailed the wide range of terminology used to define the various components of faults and fault zones, highlighting the potential uncertainty in determining the boundaries of a fault zone. Furthermore, even a well-mapped fault zone may have variability in thickness along its length. In other cases, the fault zone thickness may be unobserved (e.g., modelling from a regional geologic map) and must be approximated from available prior information.

When fault thickness is measured directly, normal or uniform distributions are appropriate for characterizing the uncertainty stemming from natural variability and inconsistent definition of the fault zone boundaries. Lacking direct observations of fault zone thickness, prior knowledge of the regional displacement of faults can provide an approximation of fault zone thickness by applying published relationships between fault displacement and fault zone thickness (Childs et al., 2009; Torabi et al., 2019). The relationships are relatively independent of fault type, and have been demonstrated for faults in sedimentary, carbonate and crystalline rocks. Uncertainty exists in both the displacement used, as well as the power law curve-fit parameters used in the relationship. Conservative modelling of displacement uncertainty should use a bounded uniform distribution, while the uncertainty of curve-fit parameters can be approximated from the standard error of the fit.

3. UNCERTAINTY ASSESSMENT

Uncertainty assessment of the 3D geologic model consists of three steps following characterization of the input uncertainties: Monte Carlo simulation, uncertainty propagation and uncertainty quantification.

3.1 Simulation

Simulation from the probability distributions described in Section 2 is carried out using open-source programming distributions from the R and Python environments. Particularly, PyMC3 (Salvatier et al., 2016) is available for the majority of continuous and discrete probability distributions, while Rfast (Papadakis et al., 2018) provides additional functionality for simulating from spherical distributions. The normal and uniform distributions implemented in PyMC3 take advantage of the efficient No-U-Turn Sampler (NUTS) (Hoffman & Gelman, 2014). The Bingham distribution implemented in Rfast uses an acceptance-rejection sampling method put forward by Kent et al. (2013**)**.

Following simulation, additional processing steps may be required to translate the sampled uncertainties back into the space of the geologic modelling inputs. The structural orientations drawn from the Bingham distribution are rotated to the appropriate orientation using a series of spherical rotations based on the Euler-Rodrigues formula (Dai, 2015). Additionally, the sampled vertical termination depths are matched to pre-defined termination surfaces as required by the proposed geologic modelling workflow. The interval at which to define termination surfaces should be determined based on the scale of the project.

3.2 Uncertainty Propagation and Quantification

The set of perturbed inputs are used to generate realizations of the initial geologic model from which the original inputs were drawn. This process, implemented in Leapfrog Works with custom back-end support, takes advantage of automation provided by implicit geologic modelling algorithms to propagate the input perturbations into the geologic model. The resultant set of model realizations ($i = 1{:}n$) is discretised into a grid of cells at a user-defined resolution to evaluate the probability of occurrence (P_c) of the fault zone lithology at each cell, c (Eq. (5)).

$$P_c = \frac{\sum_{i=1}^{n} Fault\ zone=1}{n} \tag{5}$$

This step is the most computationally expensive, taking orders of magnitude more time to process than the initial input perturbation. Determining the appropriate number of model realizations and block model resolution required for accurately capturing the uncertainty of the geologic model at the scale of the project is an essential decision. In this study, approximately four times increase in total processing time was incurred from both a reduction in block model resolution by eight (doubled in x, y and z) or a three-fold increase in model realizations. Processing times are expected to vary based on computer specifications. The method implemented in this study is considered a proof of concept, with future work focusing on optimizing processing speed and efficiency to develop an uncertainty assessment tool that can be added fluidly into existing, iterative modelling workflows.

Following the evaluation of the probability of occurrence, information entropy is calculated to relate the likelihood of fault zone occurrence to a meaningful measure of model uncertainty (Eq. (6)) (Wellmann & Regenauer-Lieb, 2012).

$$H_c = -P_c \log(P_c) \tag{6}$$

For a 1-bit system (i.e., fault zone vs. intact rock) the logarithm used is of base two and information entropy ranges from 0 to 1, varying non-linearly with respect to the likelihood. Information entropy is maximal when the probability of occurrence is 0.5 (i.e., model accuracy is equivalent to a random guess), providing a measure of model uncertainty rather than model likelihood. The importance of using uncertainty rather than likelihood has been emphasized in recent works regarding risk-based analysis in tunnelling projects (Xia et al., 2017). In order to better represent the uncertainty conveyed by information entropy, use of a non-linear colormap is proposed (Figure 4). The rationale behind the new colormap is to represent likelihood of 0.5 and entropy of 1 with similar colours while minimizing confusion regarding moderate entropy values which correspond with extremely low (or high) likelihood values (e.g., $H_c = 0.3 \sim P_c = 0.05$ *or* 0.95).

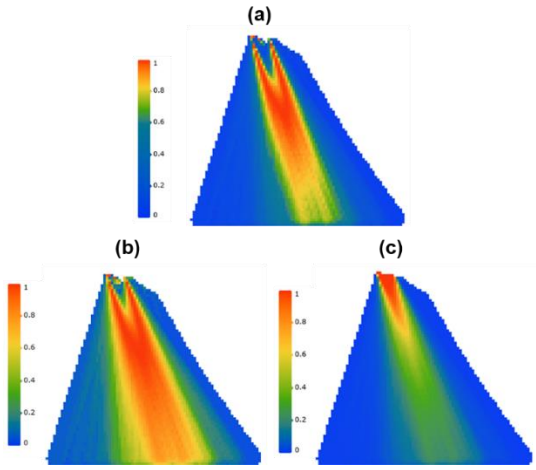

Figure 4. Recommended improvement to the entropy colormap (a) compared with a linear colormap (b) and likelihood (c).

4. CASE STUDY

Uncertainty assessment of a geologic model containing a single fault zone intersecting a tunnel alignment (Figure 5) was carried out to demonstrate the efficacy of the proposed approach. The data in the model is taken from a real tunnelling project, the Eisenhower-Johnson memorial tunnels (EJMT) in Colorado, USA. The project is a pair of 2.6 km mountain tunnels through uplifted crystalline rocks of the Rocky Mountains. The rocks have experienced a series of deformations, most recently the Laramide orogeny (70–40 Ma), resulting in pervasive brittle fault zones (Robinson et al., 1974).

The specific considerations for uncertainty of the input data are addressed and propagated into the geologic model, observing the relative contribution of each input to the resultant geologic model uncertainty. Three hundred model realizations were computed and analysed for visualization of model uncertainty at a 5 x 5 x 5 m resolution.

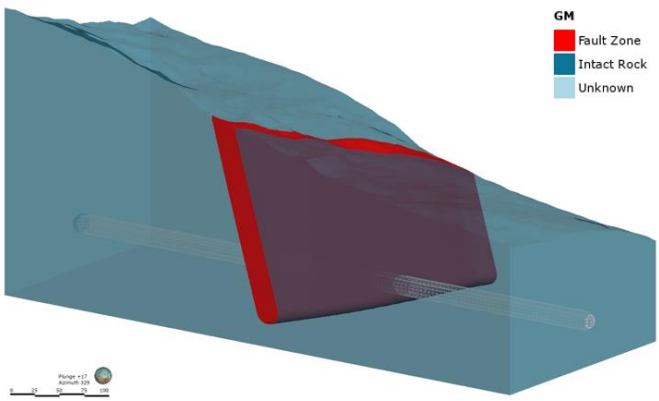

Figure 5. Initial geologic model depicting a single fault zone intersecting a tunnel alignment (grey outline).

4.1 Surface Trace

The surface trace used for modelling was derived from a scanned, historic geologic map, mapped at a 1:12,000 scale (Robinson et al., 1974). Uncertainty sources affecting the surface trace was characterized as described in Section 2.4.1 and used to perturb the input surface trace. Rather than perturbing each node of the surface trace independently, which produces a jagged shape, the polyline was perturbed independently at each end point and linearly interpolated, resulting in a smoothly altered shape and/or location of the trace. Figure 6 describes the parameters used for surface trace uncertainty along with visualizations of the generated realizations (a) and joint posterior probabilities (b).

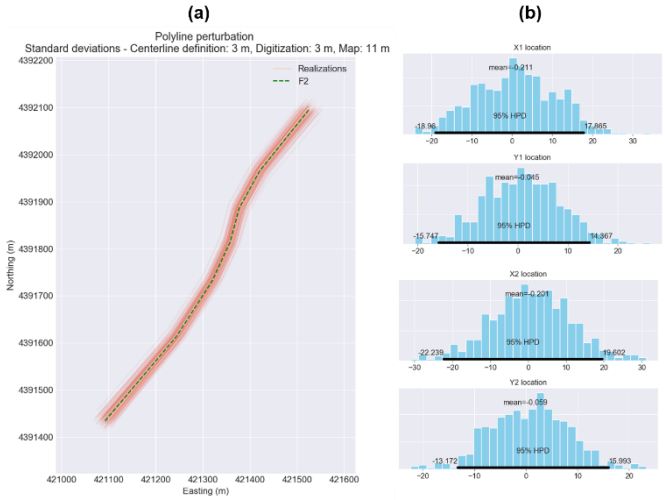

Figure 6. Surface trace perturbation realizations (a) and joint posterior probabilities (b) for the modelled fault zone.

4.2 Structural Orientation

The geologic map available from the EJMT project lacked specific information on the orientation of fault zones above the tunnel. While the strike was defined by the surface trace with a variability of approximately 15°–20°, dip had to be estimated from regional structural analysis which revealed that the majority of faults in the locality were steeply dipping from 60°–90°, primarily towards the east side. This information was used to characterize an anisotropic Bingham distribution (Figure 7).

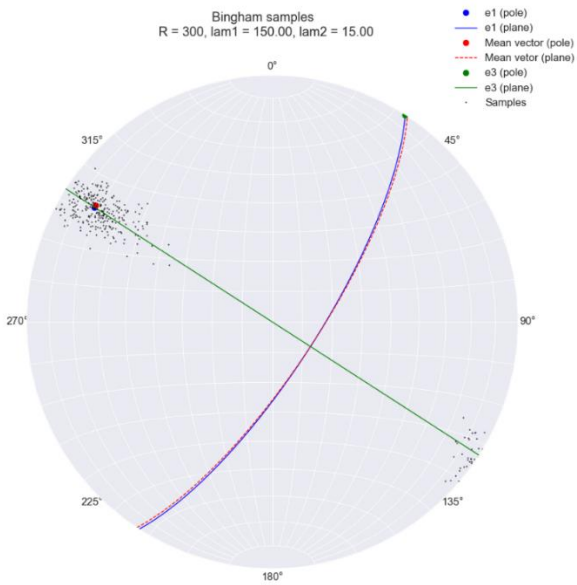

Figure 7. Perturbed orientations for the modelled fault zone sampled from an anisotropic Bingham distribution.

4.3 Vertical Termination Depth

Given the crystalline rock setting of the EJMT locality, the aspect ratios expected are on the lower range of typical values. A range of 1.5 to 5 was chosen as an initial estimate of an appropriate aspect ratio for the site geology. In the future, additional data added to the model (e.g., from the tunnel alignment) will be used to invalidate this assumption if necessary. Figure 8 displays the sampled and discretised termination depths along with the posterior probabilities.

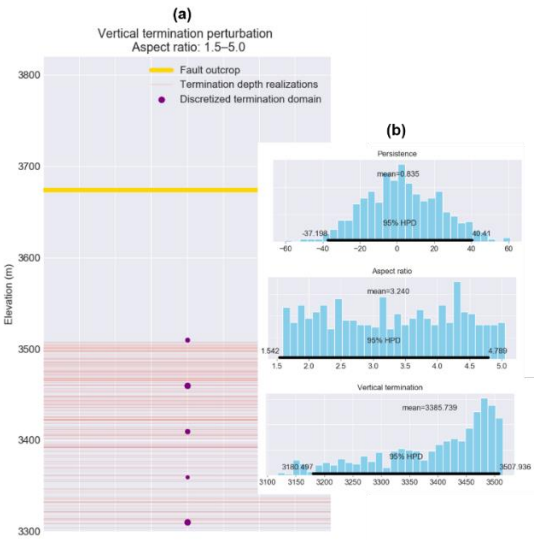

Figure 8. Sampled termination depths (a) and posterior probabilities (b) for the modelled fault zone.

4.4 Fault Zone Thickness

The thickness of fault zones provided in the EJMT dataset were noted merely as being from 5 – 50 feet (1.5 to 15 meters). Rather than model directly with a uniform distribution, a conservative estimate towards the high range of the provided information was used to model fault thickness uncertainty using a normal distribution. The modified uncertainty accounts for the original estimate in addition to uncertainties associated with the original map's interpretation of fault zone boundary locations and natural thickness variability. The realizations and posterior probabilities are shown in Figure 9.

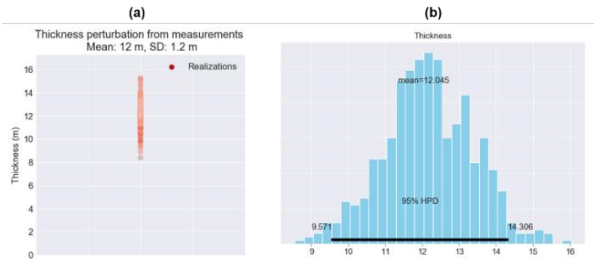

Figure 9. Thickness perturbation samples (a) and posterior probabilities (b) for the modelled fault zone.

4.5 Model Uncertainty

The uncertainty of each individual input was propagated into the geologic model independently and then the joint uncertainty of the geologic model based on simultaneous perturbation of each input was assessed (Figure 10).

Sensitivity of the combined geologic model uncertainty is dominated by orientation and termination effects in the subsurface and polyline perturbations at the surface. The combined model uncertainty is heavily dependent on the relative magnitude of individual input uncertainties. The observed sensitivity to orientation is an example of this as the EJMT dataset was most lacking in terms of the structural orientation of mapped fault zones. While the demonstrated termination uncertainty does not affect the proposed tunnel alignment, it is clearly a significant contributor to the combined model uncertainty at depth; slight changes in the believed aspect ratio range could result in terminations of the fault zone above or below the tunnel alignment. Controlling the vertical termination depth allows for a more realistic approach to modelling subsurface fault zones than the potentially overly conservative interpretation with all fault zones cutting the entire model. Finally, the sensitivity to polyline perturbations is expected to increase in modelling scenarios where the proposed tunnel alignment is not centred along the fault trace, leading to increased impact on the extrapolated fault surface.

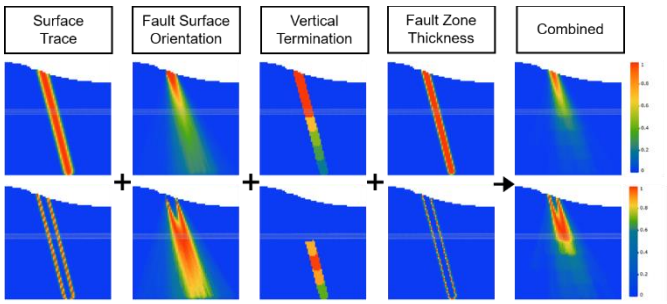

Figure 10. Likelihood (top) and information entropy (bottom) of the modelled fault zone for independent and combined input uncertainties. Tunnel alignment shown in grey outline.

It was also observed that the anisotropic Bingham distribution outperformed the accuracy of a comparable, isotropic distribution for modelling structural uncertainty. Modelling fault surfaces from a polyline trace (explicit constraint) and a structural orientation (implicit constraint) results in inaccurate geometry when the two inputs are in disagreement (e.g., structural orientation azimuth differs greatly from azimuth of polyline trace). Figure 11 demonstrates the overestimation of the dip of a modelled fault surface by 5° caused by a 30° deviation between the polyline azimuth and structural orientation azimuth. In this study, the anisotropic Bingham distribution preserved the appropriate uncertainty in dip angle (+/-30°) while restricting the azimuth uncertainty to the observed variability in the surface trace (+/-15°), minimizing skewing of the modelled fault surface as compared to the isotropic Bingham distribution with equal uncertainty in the dip angle and dip azimuth.

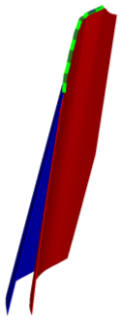

Figure 11. Overestimation of the dip of a modelled fault surface (red) when structural orientation is not in agreement with polyline azimuth.

5. CONCLUSIONS

This paper proposes a novel formulation for uncertainty assessment of fault zones intersecting tunnel alignments based on the MCUP method. The proposed formulation focuses on sources of geologic uncertainty stemming from observations, interpretations and the use of prior knowledge. These sources of geologic uncertainty are often overlooked, and potentially have a greater impact on the resultant 3D geologic model than spatial variability (Bond, 2015; Caers, 2011). The method is demonstrated on data from the EJMT project – roadway tunnels constructed in the Rocky Mountains of Colorado, USA – demonstrating how the general framework is applied to the unique considerations of a specific dataset including geologic setting and data availability.

Several improvements to previous MCUP formulations are demonstrated. A revised, non-linear colormap for communicating uncertainty using information entropy of a binary system (i.e., fault zone vs. intact rock) is proposed which highlights the high uncertainty around the boundary of modelled structures (Figure 4). The general Bingham distribution has also been implemented to overcome limitations from the reliance on isotropic, spherical distributions for characterizing structural orientation data, including difficulty characterizing disparate knowledge about the dip azimuth and dip angle of a fault without compromising the accuracy of the modelled

structure (Figure 11). The method and rationale for parameterizing pieces of geologic prior knowledge to assess the impact of subjective interpretations on geologic model uncertainty is demonstrated, using established empirical relationships such as the theory of the fault ellipse (Section 2.2.3).

Several recommendations are made to future modellers, including the importance of selecting an appropriate number of realizations and model resolution to balance processing time with quality of the uncertainty assessment. The number of realizations used is a balance between the ability for the Monte Carlo sampling to effectively explore the entire uncertainty space of each modelling input and the processing time of model creation. In the case study presented in Section 4, 300 realizations were used for efficiency (~3 hours), though the ideal number of model realizations is estimated to be approximately 1000 (~10 hours). The model resolution used for evaluation should be approximately less than or equal to half of the expected feature size to minimize pixelization in the calculated entropy. Future work will involve improving processing efficiency.

A natural extension of the forward-modelling based uncertainty assessment produced by the MCUP formulation is incorporating new information using Bayesian inference. In this manner, the parameters and prior knowledge used in initial modelling are validated (or rather, invalidated **(**Tarantola, 2006)) against the new observations, and the prior uncertainty envelopes used are updated using Bayes Theorem.

6. ACKNOWLEDGEMENTS

Support from the University Transportation Center for Underground Transportation Infrastructure (UTC-UTI) at the Colorado School of Mines for funding this research under Grant No. 69A3551747118 from the U.S. Department of Transportation (DOT) is gratefully acknowledged. Steve Harelson (stephen.harelson@state.co.us) from the Colorado Department of Transportation (CDOT) is gratefully acknowledged for providing access to data from the Eisenhower-Johnson Memorial Tunnels project. Dr. Rose Pearson (rose.pearson@seequent.org) from Seequent is gratefully acknowledged for providing custom back-end support for implementing the proposed uncertainty modeling in Leapfrog Works.

7. REFERENCES

Aydin, O., & Caers, J. K. (2017). Quantifying structural uncertainty on fault networks using a marked point process within a Bayesian framework. *Tectonophysics*, *712–713*, 101–124. https://doi.org/10.1016/j.tecto.2017.04.027

Barnett, J. A. M., Mortimer, J., Rippon, J. H., Walsh, J. J., & Watterson, J. (1987). Displacement Geometry in the Volume Containing a Single Normal Fault. *American Association of Petroleum Geologists Bulletin*, *71*(8), 925–937.

Bingham, C. (1964). Distributions on the Sphere and on the Projective Plane, 186. Retrieved from Bingham1964.pdf

Bond, C. E. (2015). Uncertainty in structural interpretation: Lessons to be learnt. *Journal of Structural Geology*, *74*, 185–200. https://doi.org/10.1016/j.jsg.2015.03.003

Caers, J. (2011). *Modeling Uncertainty in the Earth Sciences*. https://doi.org/https://doi.org/10.1002/9781119995920.ch8

Cherpeau, N., Caumon, G., & Lévy, B. (2010). Stochastic simulations of fault networks in 3D structural modeling. *Comptes Rendus - Geoscience*, *342*(9), 687–694. https://doi.org/10.1016/j.crte.2010.04.008

Childs, C., Manzocchi, T., Walsh, J. J., Bonson, C. G., Nicol, A., & Schöpfer, M. P. J. (2009). A geometric model of fault zone and fault rock thickness variations. *Journal of Structural Geology*, *31*(2), 117–127. https://doi.org/10.1016/j.jsg.2008.08.009

Dai, J. S. (2015). Euler – Rodrigues formula variations , quaternion conjugation and intrinsic connections. *Mechanism and Machine Theory*, *92*, 144–152. https://doi.org/10.1016/j.mechmachtheory.2015.03.004

Fisher, N. I., Lewis, T., & Embleton, B. J. J. (1987). *Statistical analysis of spherical data*. Cambridge University Press.

Hoffman, M. D., & Gelman, A. (2014). The no-U-turn sampler: Adaptively setting path lengths in Hamiltonian Monte Carlo. *Journal of Machine Learning Research*, *15*, 1593–1623.

Kent, J. T., Ganeiber, A. M., & Mardia, K. V. (2013). A new method to simulate the Bingham and related distributions in directional data analysis with applications, 1–16. Retrieved from http://arxiv.org/abs/1310.8110

Pakyuz-Charrier, E., Lindsay, M., Ogarko, V., Giraud, J., & Jessell, M. (2018). Monte Carlo simulation for uncertainty estimation on structural data in implicit 3-D geological modeling, a guide for disturbance distribution selection and parameterization. *Solid Earth*, *9*, 385–402. https://doi.org/10.5194/se-9-385-2018

Papadakis, M., Tsagris, M., Dimitriadis, M., Fafalios, S., Tsamardinos, I., Fasiolo, M., … Lakiotaki, K. (2018). Package 'Rfast.' Retrieved from https://rfast.eu

Peacock, D. C. P., Nixon, C. W., Rotevatn, A., Sanderson, D. J., & Zuluaga, L. F. (2016). Glossary of fault and other fracture networks. *Journal of Structural Geology*, *92*, 12–29. https://doi.org/10.1016/j.jsg.2016.09.008

Robinson, C. S., Lee, F. T., Scott, J. H., Carroll, R. D., Hurr, R. T., Richards, D. B., … Abel, J. F. (1974). Engineering Geologic, Geophysical, Hydrologic, and Rock-Mechanics Investigations of the Straight Creek Tunnel Site and Pilot Bore, Colorado. In *USGS Numbered Series*. Washington, D.C.: United States Government Printing Office. https://doi.org/https://doi.org/10.3133/pp815

Salvatier, J., Wiecki, T. V, & Fonnesbeck, C. (2016). Probabilistic programming in Python using PyMC3. *PeerJ Computer Science*, *2*(55), 1–24. https://doi.org/10.7717/peerj-cs.55

Schultz, R. A., & Fossen, H. (2001). Displacement-length scaling in three dimensions : The importance of aspect ratio and application to deformation bands. *Journal of Structural Geology*, *24*(9), 1389–1411. https://doi.org/10.1016/S0191-8141(01)00146-8

Tarantola, A. (2005). *Inverse Problem Theory and Methods for Model Parameter Estimation*. Society for Industrial and Applied Mathematics. https://doi.org/10.1137/1.9780898717921

Tarantola, Albert. (2006). Popper, Bayes and the inverse problem. *Nature Physics*, *2*(August), 492–494.

Torabi, A., Alaei, B., & Libak, A. (2019). Normal fault 3D geometry and displacement revisited: Insights from faults in the Norwegian Barents Sea. *Marine and Petroleum Geology*, *99*(April 2018), 135–155. https://doi.org/10.1016/j.marpetgeo.2018.09.032

Torabi, A., Johannessen, M. U., & Ellingsen, T. S. S. (2019). Fault Core Thickness: Insights from Siliciclastic and Carbonate Rocks. *Geofluids*, *2019*, 1–24. https://doi.org/10.1155/2019/2918673

Wellmann, F., & Caumon, G. (2018). *3-D Structural geological models: Concepts, methods, and uncertainties*. *Advances in Geophysics* (1st ed., Vol. 59). Elsevier Inc. https://doi.org/10.1016/bs.agph.2018.09.001

Wellmann, J. F., & Regenauer-Lieb, K. (2012). Uncertainties have a meaning: Information entropy as a quality measure for 3-D geological models. *Tectonophysics*, *526–529*, 207–216. https://doi.org/10.1016/j.tecto.2011.05.001

Wood, R., & Curtis, A. (2004). Geological prior information, and its application to geoscientific problems. In *Geological Prior Information: Informing Science and Engineering* (Vol. 239, pp. 1–14). https://doi.org/10.1144/GSL.SP.2004.239.01.01

Xia, Y., Xiong, Z., Dong, X., & Lu, H. (2017). Risk Assessment and Decision-Making under Uncertainty in Tunnel and Underground Engineering. *Entropy*, *19*, 549. https://doi.org/10.3390/e19100549

Zhong-Zhong, C. (1995). *The estimation of digitizing error and its propagation results in GIS and application to habitat mapping*. University of Massachusetts Amherst.